The EMBO Journal (2009) 28, 2360–2373 | © 2009 European Molecular Biology Organization | Some Rights Reserved 0261-4189/09
www.embojournal.org

THE EMBO JOURNAL

EMBO open

Numb regulates cell–cell adhesion and polarity in response to tyrosine kinase signalling

Zezhou Wang, Shelley Sandiford, Chenggang Wu and Shawn Shun-Cheng Li*

Department of Biochemistry and the Siebens-Drake Medical Research Institute, Schulich School of Medicine and Dentistry, University of Western Ontario, London, Ontario, Canada

Epithelial-mesenchymal transition (EMT), which can be caused by aberrant tyrosine kinase signalling, marks epithelial tumour progression and metastasis, yet the underlying molecular mechanism is not fully understood. Here, we report that Numb interacts with E-cadherin (E-cad) through its phosphotyrosine-binding domain (PTB) and thereby regulates the localization of E-cad to the lateral domain of epithelial cell–cell junction. Moreover, Numb engages the polarity complex Par3–aPKC–Par6 by binding to Par3 in polarized Madin-Darby canine kidney cells. Intriguingly, after Src activation or hepatocyte growth factor (HGF) treatment, Numb decouples from E-cad and Par3 and associates preferably with aPKC–Par6. Binding of Numb to aPKC is necessary for sequestering the latter in the cytosol during HGF-induced EMT. Knockdown of Numb by small hairpin RNA caused a basolateral-to-apicolateral translocation of E-cad and β-catenin accompanied by elevated actin polymerization, accumulation of Par3 and aPKC in the nucleus, an enhanced sensitivity to HGF-induced cell scattering, a decrease in cell–cell adhesion, and an increase in cell migration. Our work identifies Numb as an important regulator of epithelial polarity and cell–cell adhesion and a sensor of HGF signalling or Src activity during EMT.

The EMBO Journal (2009) **28,** 2360–2373. doi:10.1038/emboj.2009.190; Published online 16 July 2009
Subject Categories: cell & tissue architecture; signal transduction
Keywords: cell polarity; E-cadherin; EMT; Numb; tyrosine kinase

Introduction

The transition of epithelial cells to a mesenchymal phenotype is a fundamental process governing morphogenesis in multicellular organisms and underlies progression and metastasis of epithelial cancers (Guarino, 2007; Guarino *et al*, 2007; Hugo *et al*, 2007; Mandal *et al*, 2008). Epithelial-mesenchymal transition (EMT) consists of several steps: the dissolution of tight junctions (TJs), loss of cell–cell adhesion, loss of apico–basal polarity, reorganization of the actin cytoskeleton and an increase in cell motility (Guarino, 2007; Guarino *et al*, 2007; Hugo *et al*, 2007; Levayer and Lecuit, 2008; Mandal *et al*, 2008). Polarized epithelial cells contain both TJs and adherens junctions (AJs) (Gumbiner, 2005; Shin *et al*, 2006; Wang and Margolis, 2007). TJs are formed by the transmembrane proteins occludin and claudin, and the cytoplasmic proteins ZO-1, -2 and -3 (Hartsock and Nelson, 2008). The evolutionarily conserved Par3–Par6–aPKC polarity complex has an essential function in the establishment of the TJ (Macara, 2004; Margolis and Borg, 2005; Suzuki and Ohno, 2006). Par6 contains an N-terminal Phox-Bem1 (PB1) domain that binds to the PB1 domain of aPKC through heterodimerization, a C-terminal PDZ domain that binds the Par3 PDZ domain, and a Cdc42–Rac interaction binding motif that recruits the small GTPase Cdc42 or Rac to the complex (Wang *et al*, 2004; Margolis and Borg, 2005; Wang and Margolis, 2007). The AJs are maintained by E-cadherin (E-cad), p120-catenin (p120), β-catenin and α-catenin that form a dynamically regulated complex coupled to the actin cytoskeleton (Drees *et al*, 2005; Yamada *et al*, 2005; Hartsock and Nelson, 2008). On the initiation of EMT, polarized epithelial cells gradually lose their apical–basal polarity and cell–cell junctions and acquire the characteristics of mesenchymal cells capable of migrating away from the primary site into surrounding tissues.

EMT is often induced by excessive signalling of a growth factor such as the transforming growth factor-β1 (TGF-β1), the hepatocyte growth factor (HGF) or the fibroblast growth factor (FGF), or by aberrant activation of a non-receptor protein kinases (PK) such as Src (Birchmeier *et al*, 2003; Avizienyte *et al*, 2004; Avizienyte and Frame, 2005; Wang *et al*, 2008). A long-standing question in cancer metastasis is how external stimuli-induced signals may regulate cell polarity and cell–cell adhesion to induce EMT. Recent work has begun to shed light on this important issue. For example, Par6 was shown to interact with TGF-β receptor and function as a direct substrate of TGF-βRII. Moreover, phosphorylated Par6 recruits the E3 ubiquitin ligase Smurf1 and thereby promotes localized RhoA degradation and ultimately leads to loss of TJ (Ozdamar *et al*, 2005; Bose and Wrana, 2006). The activated ErbB2 receptor tyrosine kinase was shown to signal through the polarity complex Par6–aPKC to disrupt apical–basal polarity in breast epithelial cells (Aranda *et al*, 2006). Wang *et al* identified Par3 as a substrate of c-Src or c-Yes and showed that abrogation of Par3 tyrosine phosphorylation promoted its dissociation from the LIM kinase 2 and delayed TJ assembly (Wang *et al*, 2006). These studies suggest extensive interplays between kinase signalling and cell polarity and call for further investigation into the underlying mechanism.

*Corresponding author. Department of Biochemistry, Schulich School of Medicine and Dentistry, University of Western Ontario, University of Western Ontario, London, Ontario, Canada N6A 5C1.
Tel.: +519 850 2910; Fax: +519 661 3175;
E-mail: sli@uwo.ca

Received: 18 January 2009; accepted: 5 June 2009; published online: 16 July 2009

In a proteomic screen for Numb-interacting proteins, we identified several polarity and junctional proteins, including Par3 and E-cad, that co-purified with GST-Numb-PTB (phosphotyrosine-binding), implicating Numb in cell polarity and cell–cell adhesion (data not shown). In support of this notion, Rasin *et al* have shown that Numb and Numbl (Numblike) are required for the maintenance of cadherin-based adhesion and polarity in neural progenitors (Rasin *et al*, 2007). Specifically, inactivation of Numb in these neuroepithelial cells results in a basolateral-to-apical membrane translocation of cadherin (Rasin *et al*, 2007). An interaction between Numb and E-cad has been observed both *in vitro* and in ependymal cells of the postnatal mouse brain (Kuo *et al*, 2006). Moreover, Numb was found to bind Par3 and control directional cell migration by modulating the trafficking of integrins (Nishimura and Kaibuchi, 2007). The asymmetric localization of Numb during the division of *Drosophila* neuroblasts is controlled by aPKC, which phosphorylates Numb on specific serine residues and results in its release from the apical cortex (Smith *et al*, 2007).

Here, we use the Madin-Darby canine kidney (MDCK) cell line to characterize a role for Numb in regulating epithelial polarity and cell–cell adhesion and in HGF-induced EMT. HGF engages the Met receptor, which, in turn, activates downstream signalling proteins such as the Src kinase (Ponzetto *et al*, 1994; Boyer *et al*, 1997). Activation of Src has been shown to promote E-cad phosphorylation and internalization (Fujita *et al*, 2002; Pece and Gutkind, 2002; Palovuori *et al*, 2003), whereas loss of E-cad expression or its mislocalization has been implicated in cancer progression and metastasis (Thiery and Sleeman, 2006; Jeanes *et al*, 2008; Yang and Weinberg, 2008). We show here that Numb binds to E-cad through a conserved NVYY motif in the cytoplasmic domain, but that this interaction is abolished by tyrosine phosphorylation. In the absence of a tyrosine kinase signal, Numb is associated with Par3, but on addition of HGF or the activation of Src, Numb decouples from Par3 and now binds selectively to aPKC–Par6, sequestering the latter in the cytosolic and membrane compartments during HGF-induced EMT. Using E-cad mutants and small hairpin RNA (shRNA)-mediated knockdown of Numb in MDCK cells, we further show that Numb is necessary for the proper subcellular localization of E-cad, β-catenin and the Par3–Par6–aPKC polarity proteins. Accordingly, depletion of Numb sensitizes cells to HGF-induced EMT by causing a decrease in cell–cell adhesion and an increase in cell motility.

Results

Tyrosine phosphorylation negatively regulates binding of the Numb PTB domain to an NVYY motif in E-cad

To understand the function of the Numb–E-cad interaction in epithelial cells, we first established by co-immunoprecipitation (co-IP) that endogenous Numb and E-cad interacted in MDCKII cells (Figure 1A). To determine whether the Numb–E-cad interaction was modulated by tyrosine kinase signalling, cells were either incubated with the phosphatase inhibitor pervanadate or transfected with a *v-src*-expressing vector, both of which significantly enhanced the tyrosine phosphorylation level of E-cad (Figure 1A). The phosphorylation of E-cad in *v-src*-transfected cells was not as pronounced as in pervanate-treated cells, likely due to the more specific effect of Src in comparison to pervanadate. Conversely, cells were treated with PP2, an Src-specific kinase inhibitor to suppress phosphorylation. Although the Numb–E-cad interaction was attenuated by pervanadate and completely abolished by v-Src expression, it was strengthened by PP2 treatment (Figure 1A). These data show that the Numb–E-cad interaction is negatively regulated by Src activity.

Sensitivity of the Numb–E-cad interaction to tyrosine phosphorylation of the latter prompted us to investigate a potential role for the PTB domain in regulating Numb binding to E-cad. Indeed, a GST-fused Numb-PTB domain, but not GST alone, precipitated E-cad from the MDCKII cell lysate (Figure 1B). In searching for a PTB-binding site in E-cad, we performed a multiple sequence alignment and identified a potential PTB-binding motif, NVYY, in the cytoplasmic domain of E-cad (Figure 1C). This motif is conserved in vertebrates and conforms to the canonical N[V/I][Y/F][Y/F] motif determined earlier for the Numb PTB domain (Zwahlen *et al*, 2000). To confirm this prediction, a 'peptide-walking' array (Jia *et al*, 2005) representing the cytoplasmic region of human E-cad was synthesized and probed for binding to purified Numb-PTB domain. From this experiment, we identified the peptide, DNVYY^{754}, as the minimum sequence required for binding (Figure 1D). Besides containing a canonical PTB-binding motif, NVYY, this peptide overlaps with a tyrosine triad, YYY. To evaluate the importance of tyrosine residues in PTB binding, we synthesized peptide analogs in which the triad Tyr residues were replaced, individually or in combination, by Ala, Phe or pTyr residues. Probing of the resulting peptide array by Numb-PTB revealed that the first two tyrosines in the triad were essential for binding because their respective substitution by an Ala led to a marked reduction or complete loss of affinity. Intriguingly, substitution of any Tyr residue in the triad by a pTyr abrogated binding, echoing earlier results showing an inhibitory effect of phosphorylation on the Numb–E-cad interaction. This observation is also reminiscent of the interaction between the tensin-1 PTB domain and β-integrin in which tyrosine phosphorylation of the latter had a negative effect on the interaction (McCleverty *et al*, 2007). In agreement with the peptide array results, an E-cad mutant, E-cad(3A) in which the Tyr triad was replaced by an Ala triad (i.e. YYY to AAA), failed to bind Numb, whereas the triple F mutant, E-Cad(3F) (i.e. YYY to FFF) was as effective as the wild-type (wt) E-cad in precipitating Numb (Figure 1E).

HGF signalling or Src activation regulates dynamic interactions of Numb with E-cad and components of the Par polarity complex

As E-cad can be phosphorylated at the triad tyrosines during an EMT induced by the activation of Src or a receptor tyrosine kinase (Fujita *et al*, 2002), it is likely that a dynamic Numb–E-cad interaction has a function in this process. To explore this notion, we examined, by reciprocal co-IP and western blotting, the complex of Numb and E-cad in MDCKI cells transformed by a temperature-sensitive allele of *src* (Behrens *et al*, 1993). The *ts-src*-MDCKI cells formed normal cell–cell junctions when cultured as a monolayer at the non-permissive temperature of 40°C but acquired characteristics of mesenchymal cells at the permissive temperature of 35°C when Src was expressed (Supplementary Figure S1A).

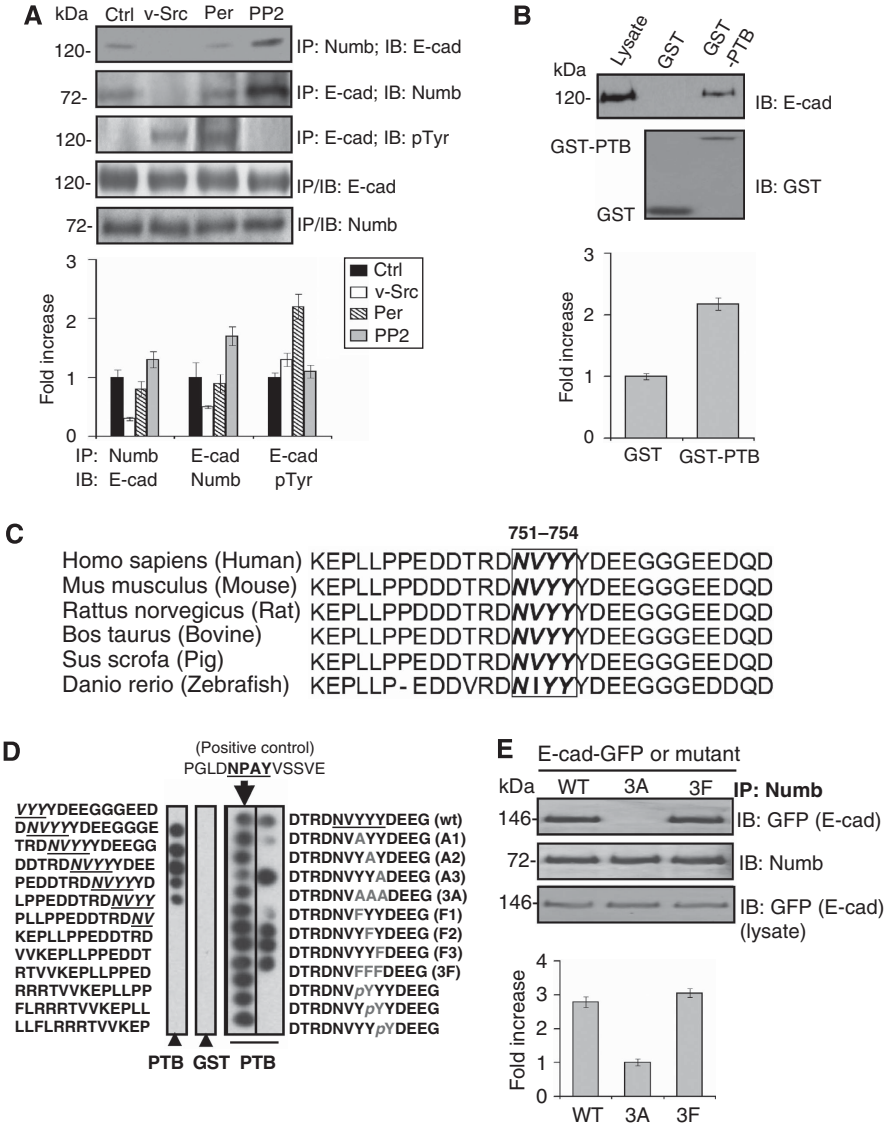

Figure 1 Numb binds to E-cadherin through its PTB domain and a conserved NVYY motif. (**A**) Reciprocal Co-IP of Numb and E-cadherin from lysate of MDCKII cells. Interaction of Numb with E-cadherin was disrupted by tyrosine phosphorylation of the latter induced by pervanadate treatment or v-Src expression. Ctrl, untreated MDCKII cells; E-cad, E-cadherin; Per, pervanadate; PP2, an Src kinase inhibitor. (**B**) The Numb PTB domain precipitated E-cadherin from MDCKII cell lysate in a GST pull-down assay. (**C**) Multiple sequence alignment revealed a highly conserved region in E-cadherins from vertebrates. The black box marks a predicted Numb PTB domain-binding motif N[V/I][Y/F][Y/F]. (**D**) Peptide array screening confirmed an NVYY motif in E-cadherin as a specific PTB-binding site. For clarity and space consideration, only a portion of the 'peptide-walking' array of the E-cadherin cytoplasmic region is shown on the left strip (the remaining array exhibited no appreciable binding to Numb PTB). GST exhibited no binding to the same strip. The left column on the strip to the right was an array of a peptide corresponding to the known Numb PTB-binding site (sequence as shown) in LNX, used as a positive control for binding and a quality control for the peptide array synthesis. The right column represents results from substitution analysis of the YYY triad at the PTB-binding site in E-cadherin. Each Tyr in the triad was replaced by an Ala, a Phe or a pTyr to evaluate its importance in PTB binding. (**E**) Binding of E-cadherin mutants to Numb. The triad YYY in E-cadherin was replaced, through site-directed mutagenesis, by AAA or FFF to generate the mutants E-cad(3A) or E-cad(3F). Wild-type E-cad and the mutants were expressed as GFP fusions in MDCKII cells and evaluated for ability to bind Numb by western blot. The bar graphs below panels of (A), (B) and (E), respectively, are data from quantitative analysis of the corresponding western blots. The error bars represent mean ± s.d.

Parallel experiments were carried out in MDCKII cells treated with HGF to mimic EMT (Balkovetz *et al*, 1997). Although both MDCKI and MDCKII are epithelial cells derived from renal tubules, the MDCKII strain exhibits less clonal variation than MDCKI (Richardson *et al*, 1981; Matter and Balda, 2003). As the MDCKII strain is used more widely in the literature, we felt it necessary to repeat the experiments done in ts-src-MDCKI cells in this strain. As shown in Figure 2A, Numb bound strongly to E-cad in *ts-src*-MDCKI cells cultured at 40°C in the absence of Src, but the interaction was abolished at 35°C when Src was expressed. Similarly, Numb was decoupled from E-cad after HGF treatment of MDCKII cells (Figure 2A). As E-cad is tyrosine phosphorylated on Src expression or HGF stimulation (Figure 2B), it is likely that phosphorylation of one or more Tyr residue at the YYY triad in E-cad abrogated its binding to Numb.

As Numb was recently shown to bind Par3 and aPKC through its PTB domain (Nishimura and Kaibuchi, 2007),

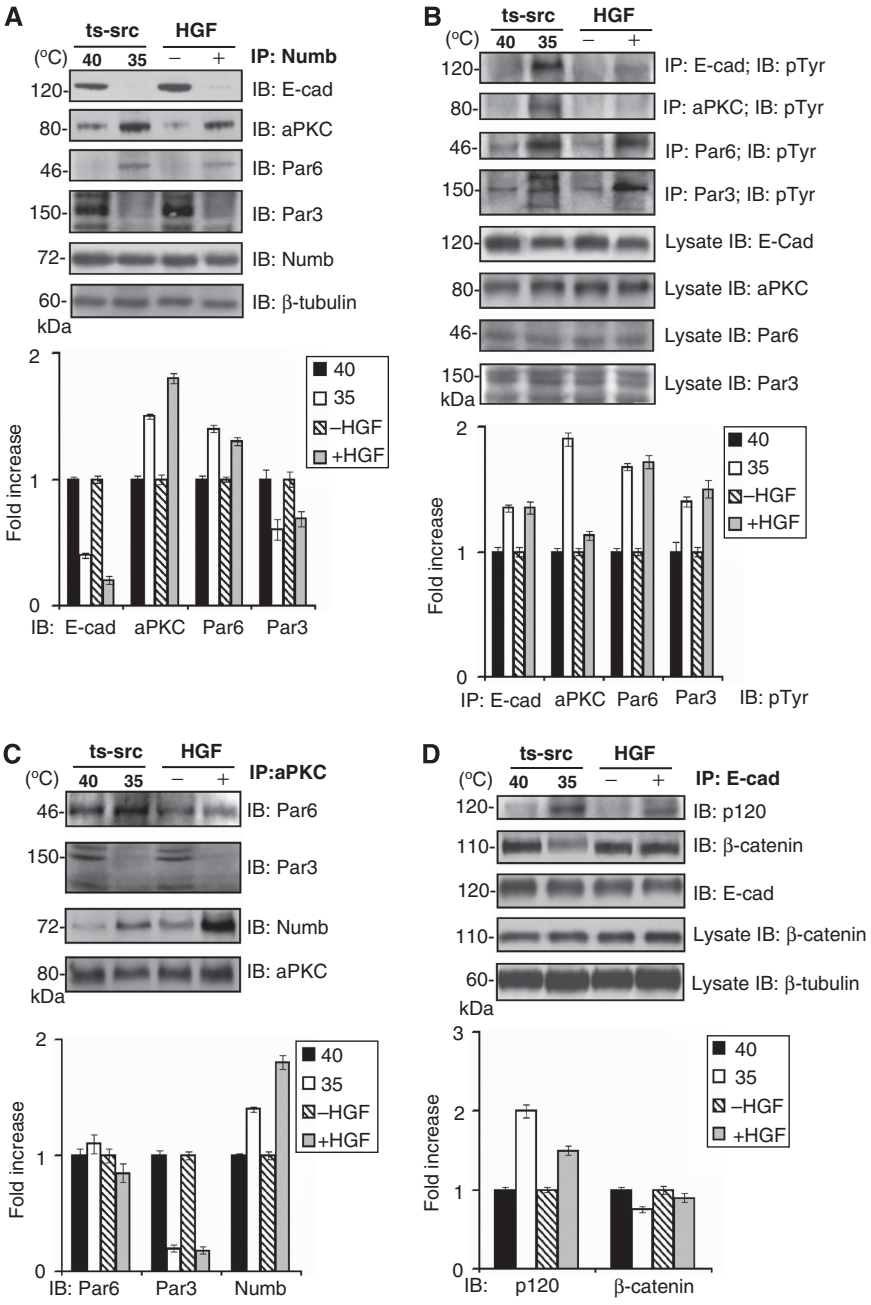

Figure 2 Src or HGF signalling regulates Numb binding to E-cadherin and the Par complex. (**A**) Co-IP of Numb with E-cadherin, aPKC, Par6 or Par3 in *ts-src*-MDCKI cells in the absence (40°C) or presence of Src (35°C), or in MDCKII cells without or with HGF treatment. (**B**) Tyrosine phosphorylation of E-cadherin, aPKC, Par6 or Par3 was examined with a specific anti-phospho-tyrosine antibody (4G10) under conditions specified in (A). E-cadhrin, aPKC, Par6 and Par3 (100 kDa, 150 kD and 180 kDa isoforms) were phosphorylated when Src was activated. In contrast, under HGF treatment, only Par6 and the 150 kD Par3 isoform were significantly phosphorylated while E-cadherin was weakly phosphorylated. (**C**) Co-IP of aPKC with Par6, Par3 and Numb, respectively, under conditions specified in (A). Both Src activation and HGF treatment promoted aPKC binding to Numb, but attenuated its interaction with Par3. (**D**) Co-IP of E-cadherin with p120-catenin and β-catenin, respectively, under conditions specified in (A). Tyrosine phosphorylation of E-cadherin enhanced its binding to p120-, but not to β-catenin. The corresponding quantification analysis of (A), (B), (C) and (D) are shown below each western blot panel. The error bars represent mean ± s.d.

we examined whether these interactions could be modulated by tyrosine kinase signalling. Indeed, Numb exhibited distinct binding preference for components of the Par3–Par6–aPKC complex in both *ts-src*-MDCKI and MDCKII cells, depending on the status of Src activation. Under basal conditions when Src was not activated, Numb bound strongly to all three isoforms of Par3 (but most strongly to the 150 kDa variant) and moderately to aPKC. Nevertheless, on Src expression or HGF treatment, the Numb–aPKC interaction was significantly augmented, whereas the Numb–Par3 interaction markedly reduced (Figure 2A and C; Supplementary Figure S1C). Furthermore, compared with a constitutive interaction between aPKC and Par6 that appeared to be independent of Src activation (Figure 2C), Par3 was dissociated from the aPKC–Par6 complex in response to Src activation (Figure 2C; Supplementary Figure S1C). In

contrast, the Numb–Par3 interaction was strengthened by PP2 treatment, but diminished in cells over-expressing v-Src (Supplementary Figure S1C and E). As Par3, Par6 and aPKC were all tyrosine phosphorylated by Src (Figure 2B), it is likely that phosphorylation played an important function in shifting their respective binding affinity and preference for one another and for Numb.

We next examined the effect of Src activation on the integrity of the cadherin complex by western blotting. E-cad bound strongly to β-catenin but only weakly to p120-catenin under basal conditions. In contrast, the E-cad–p120 interaction was enhanced in both *ts-src*-transformed (35°C) and HGF-treated cells, whereas the E-cad–β-catenin interaction was significantly attenuated in *v-src*-transformed but not in HGF-treated cells, suggesting that the activation of Src in the latter case was not as pronounced as in the former (Figure 2D). In agreement with these results, v-Src overexpression markedly augmented E-cad binding to p120-catenin, yet reduced its interaction with β-catenin. In contrast, inhibition of Src activity by PP2 completely eliminated binding of E-cad to p120-catenin, indicating that this interaction is dependent on tyrosine phosphorylation of the latter (Lilien and Balsamo, 2005) (Supplementary Figure S1D). Together, these data suggest that Src activity has an important function in regulating the integrity of the Par polarity and the cadherin complexes.

Numb is necessary for the basolateral localization of E-cad and β-catenin in epithelial cells

To investigate whether the interaction between Numb and E-cad is required for proper junctional localization of the cadherin complex, we transfected MDCKII cells with expression constructs for E-cad-GFP, E-cad-(3F)-GFP and E-cad-(3A)-GFP, respectively. As expected, E-cad-GFP localized to cell–cell junctions in polarized cells. Of the two E-cad mutants examined, E-cad-(3F)-GFP localized to the lateral membrane domain as did the wt protein. In contrast, E-cad-(3A)-GFP, which was deficient in Numb binding, was detected at the apical region of the cell–cell junction (Figure 3A and E). This suggests that a physical binding between Numb and E-cad is necessary for the proper lateral membrane localization of the latter. To interrogate whether Numb is necessary for the localization of E-cad, we generated a stable clone of MDCKII in which Numb expression was ablated by a specific shRNA (Supplementary Figure S2A and B). Confocal immunofluorescence microscopy revealed that endogenous E-cad localized to the lateral membrane of cell–cell junction as expected. Depletion of Numb by shRNA caused a basal-to-apicolateral membrane translocation of E-cad immunofluorescence (Figure 3B). However, this phenotype was completely reversed by restoration of Numb expression using a construct encoding an shRNA-resistant form of Numb (i.e. srNumb, Figure 3B and F). It should be noted that the effect of Numb knockdown on E-cad localization was less dramatic than observed for the E-cad(3A) mutant, likely due to the effect of residual Numb in the *numb*-shRNA cells. Alternatively, additional factors besides Numb may be involved in controlling endogenous E-cad localization. As the AJ is linked to the actin cytoskeleton and the reorganization of actin network underpins the formation and maturation of cell–cell contacts (Kametani and Takeichi, 2007; Hartsock and Nelson, 2008), we compared F-actin staining patterns between the control and the *numb*-shRNA MDCK cells. Numb knockdown led to a significant increase in F-actin staining compared with wt cells or cells expressing srNumb, suggesting that Numb is involved directly or indirectly in regulating actin dynamics in these cells (Figure 3B and F). Furthermore, in both *numb*-shRNA and srNumb-expressing cells, actin stain overlapped significantly with the E-cad immunofluorescence (Figure 3B). To find out whether other AJ proteins are affected by Numb depletion, we immunostained for β-catenin, a key component of the AJ. As shown in Figure 3C and G, β-catenin underwent a similar basal-to-apicolateral translocation as E-cad in *numb*-shRNA cells. This defect, however, is rescued, by expression of srNumb in these cells. Together, these data show that Numb is necessary for the proper junctional localization of E-cad and β-catenin in polarized epithelial cells. It should be pointed out that Numb depletion did not affect the formation of TJs for cells polarized on transwell filters as indicated by the apical staining of ZO-1 in *numb*-shRNA cells (Figure 3D).

As HGF treatment dissociated Numb from E-cad, we next investigated whether HGF modulated E-cad localization in *numb*-shRNA cells in comparison to in control MDCKII or cells expressing srNumb. In contrast to a tight junctional membrane staining signal for E-cad in polarized MDCKII cells, HGF treatment resulted in a punctate staining pattern for E-cad at the apicolateral membrane domain between adjacent cells and diffused cytosolic stain (Figure 4A), suggesting dissolution of the AJ. Similarly, HGF induced a redistribution of Numb from the plasma membrane to the cytosol (Figure 4A). Depletion of Numb in the *numb*-shRNA stable clones, although not affecting their ability to polarize on filters, led to an accumulation of E-cad at the apicolateral membrane domain in the absence of HGF and a redistribution of E-cad to the cytosol after HGF treatment (Figure 4B). In contrast, E-cad remained largely on the junctional membrane in cells expressing srNumb in the presence of HGF, although the immunofluorescence signal was significantly reduced in comparison to in cells without HGF treatment (Figure 4C). To find out whether Numb depletion sensitizes cells to HGF-induced EMT, we examined, by fluorescence microscopy, the localization of E-cad in subconfluent MDCKII or *numb*-shRNA cells stimulated with HGF for 0, 6, 12 or 18 h (Supplementary Figures S3 and S4). These cells were partially polarized and therefore more sensitive to HGF treatment than a monolayer of fully polarized epithelial cells. Numb depletion coincided with faster dispersion of *numb*-shRNA cells (e.g. at 6 h of HGF treatment) than control cells (e.g. at 12 h of HGF treatment) and promoted redistribution of E-cad from the membrane to the cytosol (Supplementary Figures S3 and S4).

Numb differentially regulates the subcellular localization of Par3 and aPKC–Par6 during HGF-induced EMT

Our biochemical data showed that Numb could be engaged in two distinct complexes with either Par3 or aPKC–Par6, depending on the status of Src activation. To characterize these dynamic interactions in cells undergoing EMT, we followed the subcellular localization of Par3 and aPKC, respectively, in polarized monolayer of *numb*-shRNA stable clones before or after HGF treatment. In polarized control MDCKII cells before HGF treatment, Par3 and aPKC were found mainly at the apicolateral membrane domain although

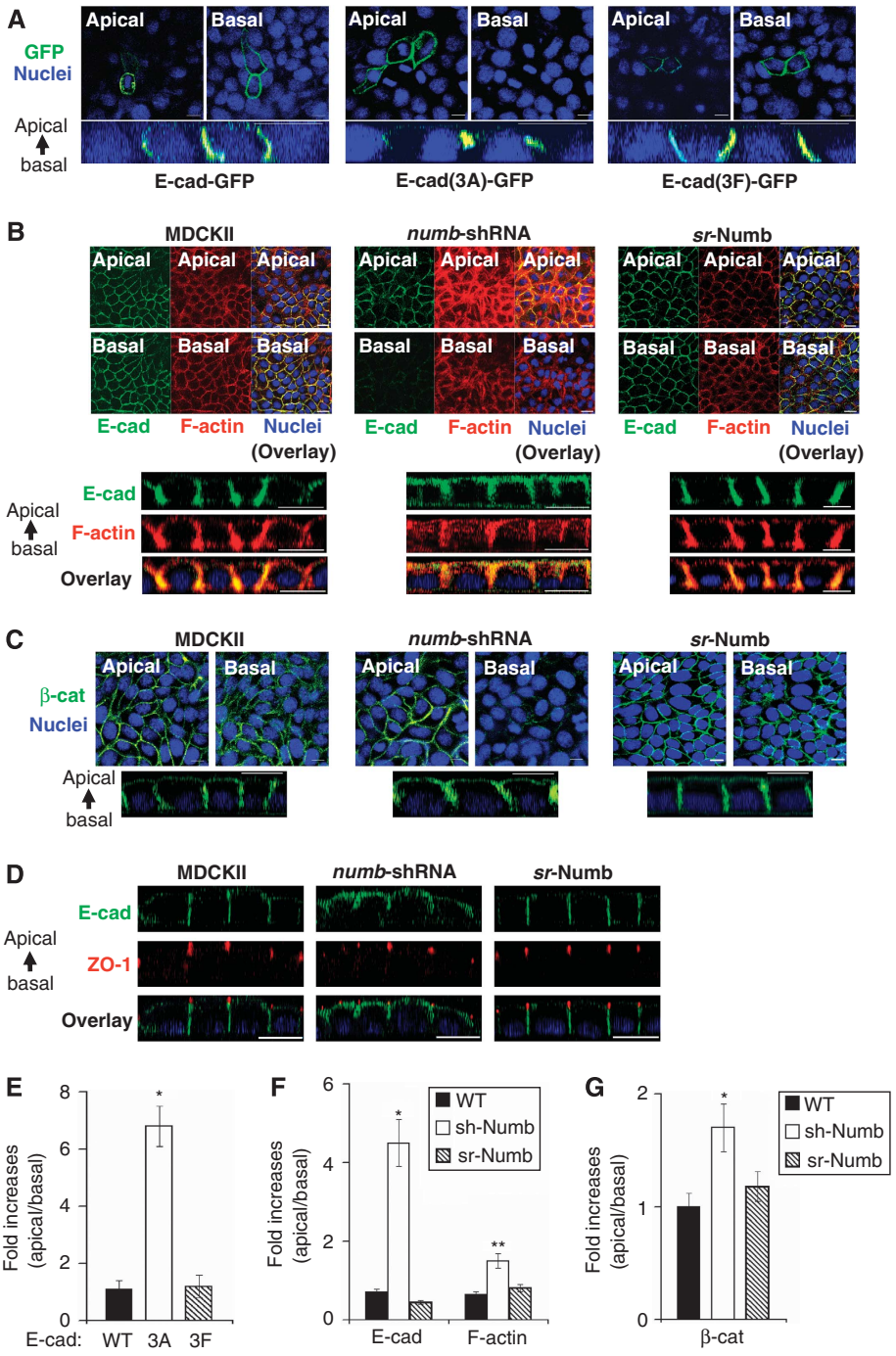

Figure 3 Numb knockdown led to aberrant localization of E-cadherin, β-catenin and F-actin. (**A**) Confocal Z-stack images of E-cad-GFP, E-cad(3A)-GFP and E-cad(3F)-GFP in transfected MDCKII cells, respectively. The panel labelled as 'apical' corresponds to an *x*/*y* section image (*x*/*y* focal plane) taken at the subapical region of the monolayer of cells (at 4 μm below the apical surface) and the panel labelled as 'basal' corresponds to the basolateral region (a section at 4 μm above the basal surface), respectively. The corresponding *x*/*z* focal plane image was shown below each *x*/*y* image set. Apical is at the top, whereas basal is at the bottom. The same convention was used throughout. Size bars represent 10 μm. GFP fluorescence is in green and nuclei are stained in blue with DAPI. (**B**) Confocal Z-stack images of E-cadherin (green) and F-actin (red) in the control MDCKII cells versus in the *numb*-shRNA or *sr*-Numb cell lines. In each panel, the E-cadherin immunostaining (green) images were shown on the left, F-actin staining (red) images in the middle and the overlaid images on the right. The corresponding *x*/*z* focal plane images were shown below the *x*/*y* images. (**C**) Confocal Z-stack images of β-catenin immunofluorescence in the control MDCKII cells versus in the *numb*-shRNA or *sr*-Numb cells shown as either *x*/*y* (top) or *x*/*z* (bottom) section. (**D**) Confocal *x*/*z* sections showing the apical translocation of E-cadherin in the control MDCKII cells versus in the *numb*-shRNA or *sr*-Numb cells. The apical surface was identified by co-staining for ZO-1. (E–G) Quantitative analysis of immunofluorescence images shown in (A), (B) and (C), respectively. Values shown are changes in fold of apical over basal immunofluorescence. $^{*}P<0.001$, $n=3$ in (**E**); $^{*}P<0.001$, $^{**}P<0.05$, $n=5$ in (**F**); $^{*}P<0.01$, $n=3$ in (**G**). The error bars represent mean ± s.d.

cytosolic staining was also detectable for Par3 (Figure 4D). HGF treatment caused translocation of Par3 to the nucleus but had little effect on aPKC localization. These immunofluorescence data were supported by cell fractionation analysis demonstrating that Par3 became nuclear after HGF treatment, whereas aPKC remained in the membranous and

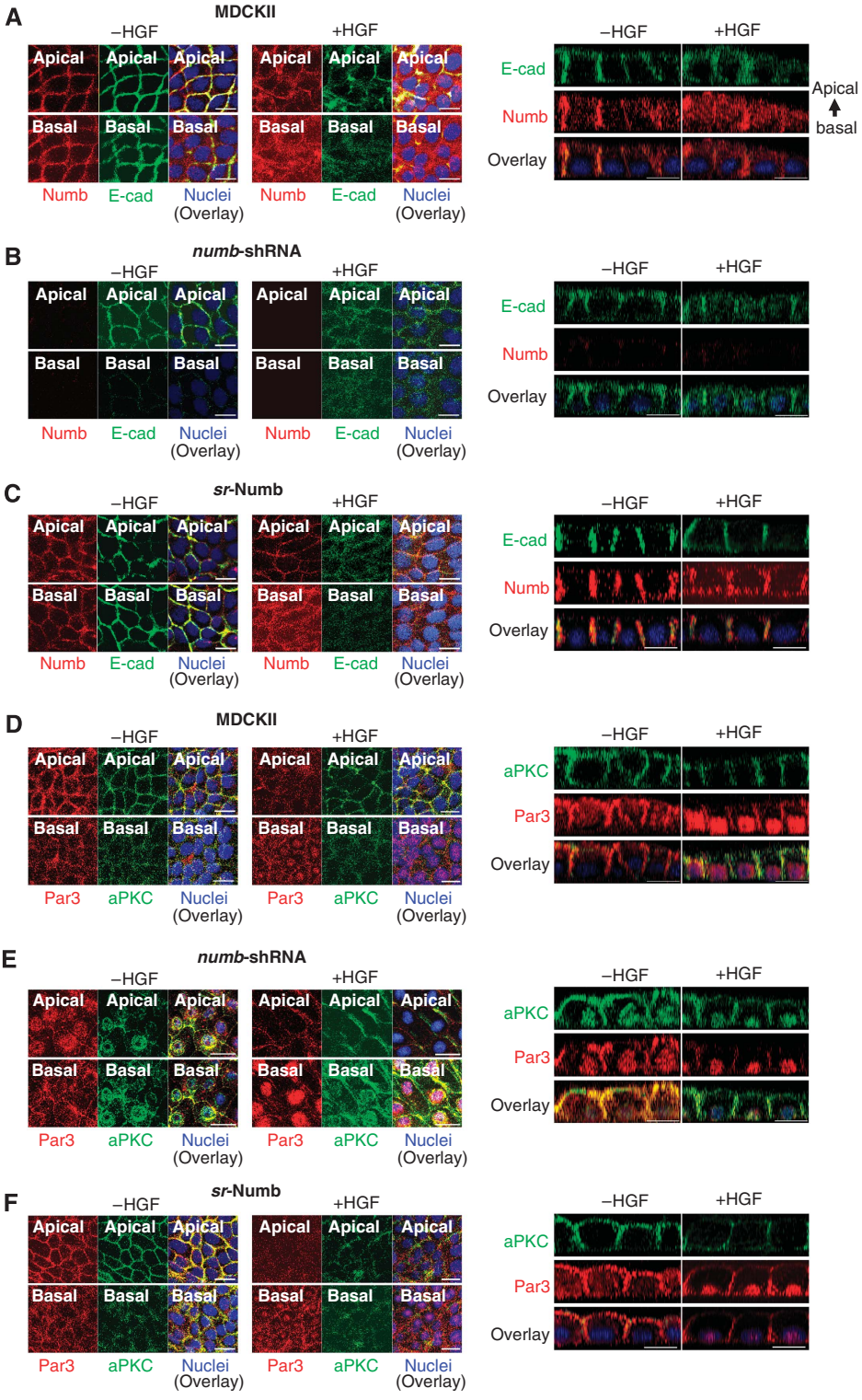

Figure 4 Numb knockdown alters the cellular localization of E-cadherin and the Par complexes in response to HGF treatment. Confocal Z-stack images of polarized MDCKII cells, *numb*-shRNA or *sr*-Numb cells co-stained for E-cadherin (green) and Numb (red) or aPKC (green) and Par3 (red) without or with HGF treatment for 18 h. Size bars represent 10 μm. (**A**) Confocal *x*/*z* and *x*/*y* section images of control MDCKII cells co-stained for E-cadherin and Numb in absence or presence of HGF. HGF treatment corresponded to weakened cell–cell junctional staining and enhanced cytosolic staining for both proteins. (**B**) Confocal *x*/*z* and *x*/*y* section images of *numb*-shRNA cells co-stained for E-cadherin and Numb under identical condition as in (A). (**C**) Confocal *x*/*z* and *x*/*y* section images of *sr*-Numb cells co-stained for E-cadherin and Numb under identical condition as in (A). (**D**) Confocal *x*/*z* and *x*/*y* section images of control MDCKII cells co-stained for aPKC and Par3. HGF treatment led to a decrease of aPKC apical membrane stain (lower panel). In contrast, a significant amount of Par3 moved into the nuclei with HGF treatment. (**E**) Confocal *x*/*z* and *x*/*y* section images of *numb*-shRNA cells co-stained for aPKC and Par3 under identical condition as in (D). Both aPKC and Par3 were found on the lateral membrane and in the nuclei already in the absence of HGF treatment. Significant overlap of the two proteins was observed with or without HGF treatment. (**F**) Confocal *x*/*z* and *x*/*y* section images of *sr*-Numb cells co-stained for aPKC and Par3 under identical condition as in (D).

cytosolic fractions (Figure 5C and D). The apparent decoupling of Par3 from aPKC was also observed in subconfluent MDCKII cells stimulated with HGF for different durations of time (Supplementary Figure S5). The partially overlapped immunofluorescence for Par3 and aPKC before HGF stimulation became discrete after exposure to HGF for 6 h when Par3 was translocated to the cytosol and nucleus while aPKC remained largely on the membrane. By 12 h, Par3 was found mainly in the nucleus whereas aPKC on the membrane and in the cytosol as the cells became more elongated and scattered (Supplementary Figure S5). These results suggest that decoupling of Par3 from aPKC and translocation of Par3 to the nucleus are early steps in HGF-induced EMT.

Compared with HGF-induced nuclear translocation of Par3 in control MDCKII cells, both Par3 and aPKC were detected in the nuclei of polarized *numb*-shRNA cells in the absence of HGF (Figure 4E). As Par3 was found in the nucleus of control cells only after HGF treatment, the change in subcellular localization for Par3 and aPKC caused by Numb depletion suggests that the *numb*-shRNA cells already acquired certain characteristics of mesenchymal cells before HGF stimulation. Indeed, stimulation of these cells by HGF for 18 h did not

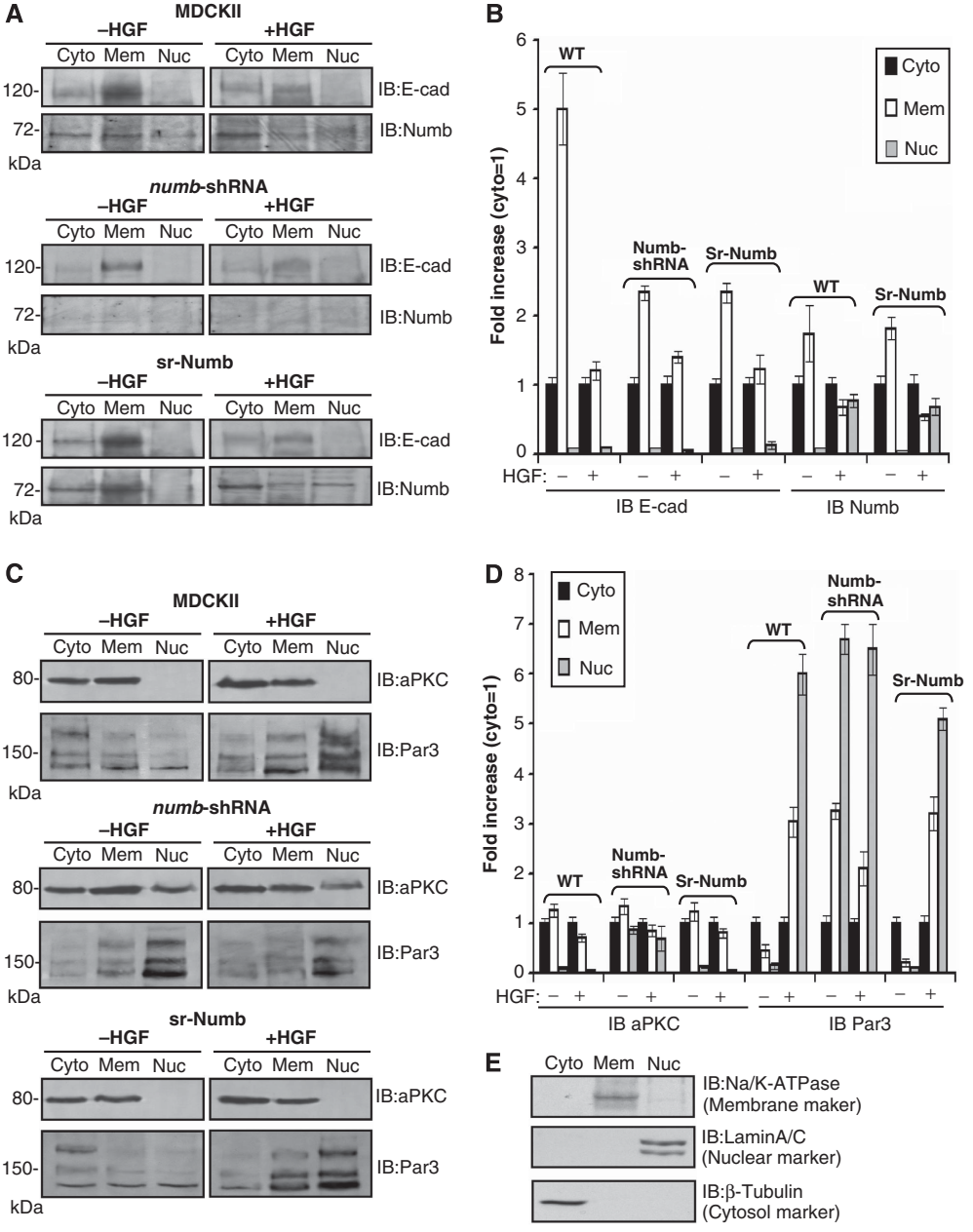

Figure 5 Changes in subcellular localization for E-cadherin, Numb, aPKC and Par3 determined by cell fractionation. Cells were lysed and separated into cytosolic (Cyto), membrane (Mem) and nuclear (Nuc) fractions and subjected to western blotting analysis using specified antibodies. (**A**) Subcellular distribution of E-cadherin and Numb in different cellular fractions without or with HGF treatment for 18 h in control MDCKII, *numb*-shRNA and sr-Numb cells. (**B**) Quantification of western blots shown in (A). The bars represent protein levels relative to that in the cytosolic fraction, set at 1. The error bars represent mean ± s.d. (**C**) Distribution of aPKC and Par3 in different cellular fractions under identical condition as in (A). (**D**) Quantification of western blots in (C). (**E**) Confirmation of fractionation by staining for specific subcellular markers.

significantly alter the subcellular localization pattern for either Par3 or aPKC (Figure 4E). We believe that the mislocalization of Par3 and aPKC in the *numb*-shRNA cells was caused specifically by the lack of Numb as restoration of Numb expression in the sr-Numb cells completely reversed this phenotype (Figure 4F). To ensure that these immunostaining signals observed for aPKC and Par3 were specific, we repeated the same experiments using anti-aPKC and anti-Par3, respectively, from different sources and obtained comparable results (Supplementary Figures S7 and S8). Moreover, the Par3 immunostaining signal was lost when the antibody was pre-incubated with a blocking antigen, suggesting that the anti-Par3 antibody used was specific (Supplementary Figures S8B and D). The immunostaining patterns were corroborated by results from western blotting of cellular fractionations. As shown in Figure 5C and D, aPKC was detected in the nuclear fraction of *numb*-shRNA cells but not control MDCK or sr-Numb cells in the absence of HGF. Similarly, Numb knockdown led to a redistribution of Par3 from the cytosolic and membranous fractions to the nuclear fraction. In agreement with immunostaining data (Figure 4), HGF stimulation did not alter the subcellular distribution of either protein significantly. To further explore the role of Numb in affecting the localization of aPKC and Par3 during EMT, we monitored their respective subcellular localization in a time-course of HGF treatment of subconfluent *numb*-shRNA cells. Compared with the control cells, the Numb-knockdown cells were more readily scattered on HGF stimulation. Moreover, prominent nuclear staining was observed for both aPKC and Par3 in the *numb*-shRNA cells, but not in the control, at 6 h of HGF treatment (Supplementary Figures S5 and S6). These results suggest that Numb may regulate EMT by controlling the subcellular localization of polarity proteins.

Depletion of Numb leads to weakened cell–cell adhesion and enhanced cell migration and proliferation

As the above biochemical and immunofluorescence data identified a critical role for Numb in the localization of both the cadherin and the Par complexes, we speculated that lack of Numb might contribute to weakened cellular junctions, reduced cell–cell adhesion, and increased cell motility. To test this hypothesis, we carried out cell aggregation and migration assays on MDCKII, *numb*-shRNA and sr-Numb cells. Although the control and sr-Numb-expressing cells formed aggregates that were not easily dispersed by pipetting, the *numb*-shRNA cells dissociate readily with the same manipulations (Figure 6A and B). To interrogate whether Numb has a function in cell migration, we performed wounding assays on these cells, respectively. Compared with the control, Numb-knockdown promoted wound healing significantly (Figure 6C and D). Boyden chamber assays also showed a marked increase in the rate of migration for the *numb*-shRNA cells. Importantly, restoration of Numb expression in the sr-Numb cells returned the migration rate to the same level as the wt cells (Figure 6E). To gauge the effect of cell proliferation on promoting cell migration, we measured the growth rate for each cell type. Numb-knockdown led to increased cell proliferation and re-expression of sr-Numb brought the cells back to their normal rate of growth (Figure 6F). It should be noted, however, that the elevated rate of cell proliferation was insufficient to account for the dramatic increase in the rate of cell migration (i.e. at 48 h post-seeding; Figure 6E and F). Therefore, it is likely that the depletion of Numb had a dual effect on MDCKII cells: increased cell proliferation and enhanced cell migration because of weakened cell–cell adhesion.

Discussion

Numb links a tyrosine kinase signal to the cadherin and Par complexes

Growth factors such as HGF, FGF and PDGF provide the necessary stimuli to trigger EMT (Birchmeier *et al*, 2003; Avizienyte *et al*, 2004; Avizienyte and Frame, 2005; Wang *et al*, 2008), but how the activation of corresponding signalling pathways regulate the transition of epithelial cells from a polarized monolayer to migratory mesenchymal cells during EMT is not fully understood. As loss of cell polarity and cell–cell adhesion are hallmarks of EMT, it is reasonable to assume that growth factor-initiated signalling events have an impact on the assembly or dissolution of the TJs and/or AJs. In keeping with this assumption, tyrosine phosphorylation of Par3 by EGF treatment or the Src family kinases (e.g. Src and Yes) has an important function in regulating epithelial TJ assembly (Wang *et al*, 2006). It has also been shown that a receptor tyrosine kinase may directly interact with components of the Par polarity complex. For instance, activated ErbB2 is capable of binding to Par6 and thereby promotes the disassociation of the Par3–aPKC–Par6–CDC42 complex to disrupt epithelial polarity (Aranda *et al*, 2006). The identification of Numb, an endocytic adaptor protein (Santolini *et al*, 2000) as a direct binder for Par3 and aPKC, and the demonstration that polarized Numb phosphorylation by aPKC contributes to directional cell migration (Nishimura and Kaibuchi, 2007) suggest that Numb is a regulator of epithelial polarity. This notion is reinforced by a recent study showing that Numb and Numbl are required for the maintenance of cadherin-based adhesion and polarity for neural progenitors (Rasin *et al*, 2007). That Numb is capable of interacting with both the Par polarity complex and E-cad raise the possibility that it may be an important regulator of both the TJ and the AJ in epithelial cells.

In the present work, we investigated the role of Numb in regulating cell polarity through the Par polarity complex and cell–cell adhesion through E-cad in the context of HGF- or Src-induced EMT of MDCK cells. Our biochemical data strongly suggest that Numb is engaged in distinct protein complexes depending on the status of Src activation. In the absence of HGF stimulation or Src activation, Numb interacts with both the Par complex through binding to Par3 and the cadherin complex through E-cad in MDCK cells. In HGF-treated or *v-src*-transformed cells, Numb is decoupled from E-cad and Par3 and binds selectively to aPKC–Par6. HGF signals through the receptor tyrosine kinase c-Met, which, in turn, activates both Src and the Erk mitogen-activated PK cascade (Ponzetto *et al*, 1994). Our observation that HGF treatment and Src activation affect the interactions mediated by Numb in a similar manner suggests that HGF signals to the TJ and AJ through the activation of Src and Src-dependent phosphorylation of junctional proteins and/or their regulators (Avizienyte *et al*, 2002; Fujita *et al*, 2002; Christiansen and Rajasekaran, 2006).

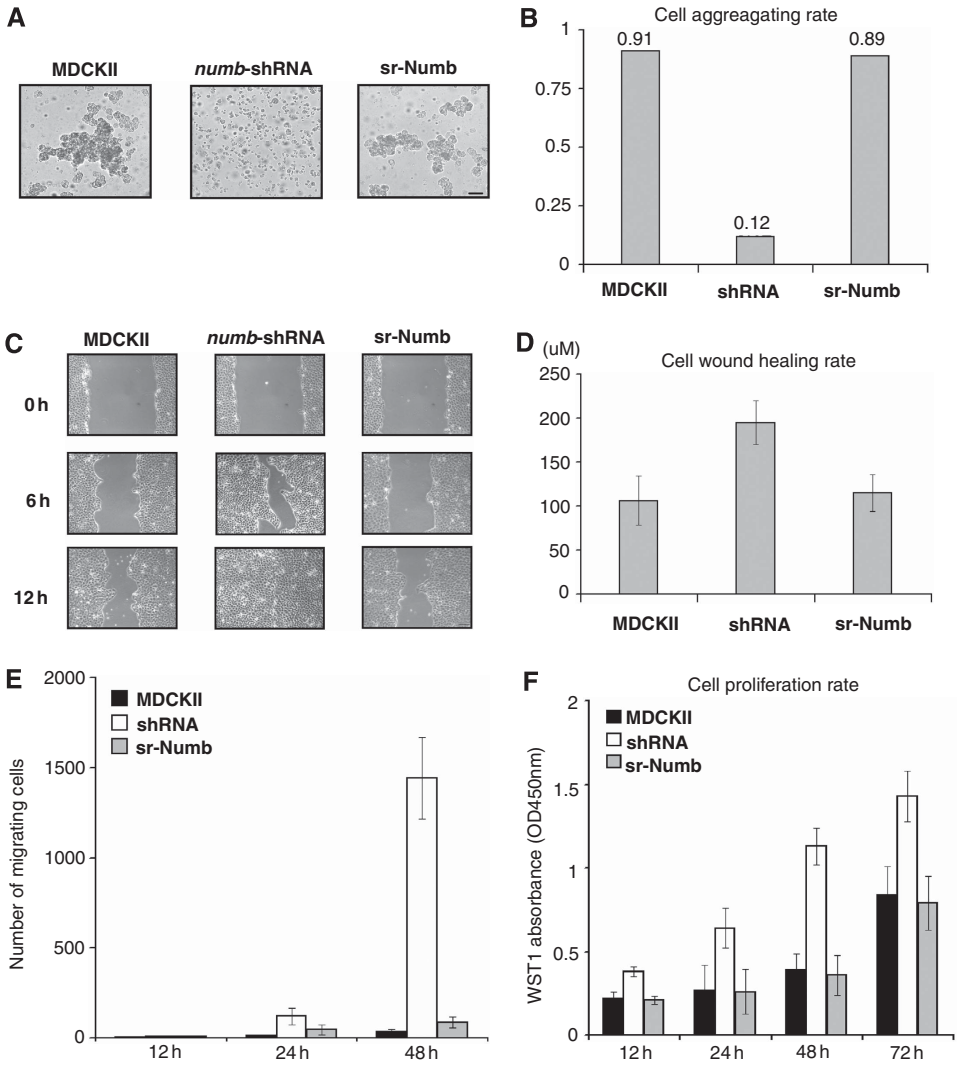

Figure 6 Numb knockdown reduced cell–cell adhesion and promoted cell migration. (**A**) Decreased adhesiveness in cells lacking Numb. Aggregation assay showed weaker cell–cell adhesion for the *numb*-shRNA cell line compared with MDCKII. However, this defect was rescued by re-expression of *sr*-Numb. The scale bar is set at 25 μm. (**B**) Quantification of cell aggregation rate shown in (A). Aggregating rate = (No−Nt)/No, where No is the number of (non-aggregated) cells used in the assay and Nt denotes the total number of particles (non-aggregated and aggregated cells) in the sample after pipetting. Data shown are representative of four independent experiments. (**C**) Numb knockdown promoted wound healing in MDCKII cells. Images were captured immediately after wounding or at 6 or 12 h afterwards. The scale bar is set at 50 μm. (**D**) Rate of wound healing for MDCKII, *numb*-shRNA or *sr*-Numb cells. The rate shown was based on 10 independent measurements. The error bars represent mean ± s.d. (**E**) Rate of cell migration measured using a Boyden chamber. Data shown were based on six independent assays. The error bars represent mean ± s.d. (**F**) Comparison of the rate of proliferation for the MDCKII, *numb*-shRNA and *sr*-Numb cells. Data shown represent three independent sets of experiments. The error bars represent mean ± s.d.

Numb has an essential function in controlling E-cad localization to the AJ

How does Numb regulate the cadherens junction in epithelial cells? We addressed this question by confocal immunofluorescence microscopy using an E-cad mutant [E-cad(3A)] defective in Numb binding and a MDCKII clone with stable shRNA-mediated Numb knockdown, respectively. Our results indicate that Numb is necessary for the basolateral membrane localization of E-cad in polarized epithelial cells. Decoupling of Numb from E-cad or depletion of Numb causes E-cad to be accumulated at the apical membrane domain in the absence of a stimulus. As Numb binds to E-cad and the two proteins colocalize in polarized MDCK cells, it is likely that a physical interaction between the two proteins is involved in targeting E-cad to the basolateral membrane in polarized epithelial cells. As Numb is capable of binding to components of the endocytosis machinery (Santolini *et al*, 2000; Dho *et al*, 2006), it may be involved in the enodocytosis of E-cad. On Src activation, E-cad becomes tyrosine phosphorylated and is decoupled from Numb. Phosphorylated E-cad has been shown to bind selectively to Hakai, an E3 ubiquitin ligase (Fujita *et al*, 2002). It is likely that Numb regulates the endocytosis and recycling of E-cad in resting epithelial cells, whereas Hakai promotes the ubiquitination and endocytosis of phosphorylated E-cad in response to Src activation. Together, Numb and Hakai may modulate dynamic changes in E-cad mediated cell–cell adhesion during normal development or EMT. This model is supported by the following considerations. First, E-cad undergoes a constant turnover at the epithelial junctional membrane. E-cad endo-

cytosis has been observed during mitosis, after HGF induced cell scattering or on depletion of extracellular calcium (Le *et al*, 1999). Second, Numb is an endocytic adaptor protein that can promote the endocytosis of a bound protein (Santolini *et al*, 2000; Dho *et al*, 2006; Nishimura and Kaibuchi, 2007). In this regard, it is interesting to note that the PTB domain of Numb binds to a YENPTY motif present in the cytoplasmic tail of APP and promotes the endocytosis of the latter (Roncarati *et al*, 2002). As E-cad binds to Numb through its PTB domain, the C-terminus of Numb is free to interact with an EH domain-containing endocytic protein and/or with AP2 (Santolini *et al*, 2000; Dho *et al*, 2006). Third, Hakai contains a PTB domain similar to that found in Cb1, also an E3 ligase. Interestingly, the Cbl PTB domain recognizes an [N/D]xxpY motif in a phosphorylation-dependent manner (Lupher *et al*, 1997); it is therefore possible that the Hakai PTB domain binds E-cad through the NVYY site on Src activation (to generate NVYpY). Indeed, Hakai has been shown to interact with E-cad in a tyrosine phosphorylation-dependent manner and thereby induce ubiquitination of E-cad. Ubiquitinated E-cad may be either degraded in the proteosome or recycled back to the membrane through the endocytic pathway (Pece and Gutkind, 2002). The potential dynamic interplay of E-cad with Numb and Hakai, which awaits further investigation, may be an important mechanism for controlling E-cad localization, trafficking and EMT under physiological and pathological conditions. Notwithstanding these considerations, however, we found that E-cad was associated with AP2 in both unstimulated and Src-activated cells (Supplementary Figure S1D), suggesting that AP2 may also directly regulate E-cad endocytosis independently of Numb.

An important yet unsolved question from this work is how knockdown of Numb causes apical accumulation of E-cad in polarized MDCK cells in the absence of a stimulus. It is likely that actin reorganization associated with Numb depletion contribute to this phenomenon.

An important function of the AJ, which is mediated by the actin cytoskeleton, is to reinforce contacts between neighbouring cells such that apical and basolateral membrane domains are maintained in polarized cells (Vasioukhin *et al*, 2000; Hartsock and Nelson, 2008). We observed a striking F-actin stress fibre-like phenotype associated in polarized *numb*-shRNA cells, which suggests abnormal cytoskeleton reorganization. Intriguingly, E-cad was found to colocalize with F-actin at the apical domain in these cells. As actin polarization is controlled by the Rho family small GTPase (Jaffe and Hall, 2005), it is possible that localized RhoA or Rac activity leads to changes in the actin cytoskeleton, which, in turn, impact on E-cad localization.

Numb regulates the TJ by sequestering Par3 and aPKC away from the nucleus

Our observation that the subcellular localization of Par3 and aPKC is altered in polarized *numb*-shRNA cells before HGF treatment strongly suggests that Numb also has an important function in regulating the stability of TJs. It is intriguing that Numb depletion caused a nuclear accumulation for aPKC independently of a kinase signal. It has been reported that aPKC may be imported into the nucleus, a process that is facilitated by tyrosine phosphorylation, in particular at the conserved Tyr263 site (White *et al*, 2002). When Numb is present, however, aPKC is retained on the membrane and in the cytoplasm regardless of Src activation or HGF treatment. This suggests that, rather than a tyrosine kinase signal, it is Numb that is responsible for sequestering aPKC away from the nucleus. In support of this notion, we found Numb bound to aPKC independently of Src activity. The interaction, however, was enhanced significantly in *v-src*-transformed or HGF-treated cells. A tighter binding of Numb to phosphorylated aPKC and the resulting sequestration of the latter in the cytosol may play an important part in delaying the process of EMT. In keeping with this consideration, Numb-depletion sensitized MDCK cells to HGF-induced EMT. Compared with aPKC, Par3 underwent nuclear translocation in both wt MDCK cells treated with HGF and in *numb*-shRNA cells. Once again, Numb has an important function in retaining Par3 in the cytosol and/or on the membrane. As the Numb–Par3 interaction was inhibited by tyrosine phosphorylation, stimulation of wt MDCK cells with HGF effectively created a scenario similar to that caused by Numb knockdown.

What is the biological significance of nuclear translocation for polarity proteins? A recent study showed that Par3 localized to the nucleus of Hela cells and bound to Ku70 and Ku80, the regulatory subunits of the DNA-dependent PK (DNA-PK) (Fang *et al*, 2007). As Par3 knockdown cells are defective in DNA repair accompanied by reduced DNA-PK activity, it was suggested that Par3 has a function in regulating DNA double strand break repair. The modular nature of Par3, which contains multiple PDZ domains and interaction motifs, suggests that additional nuclear functions may exist. As Par3 underwent nuclear translocation soon (6 h) after HGF treatment of subconfluent MDCKII cells, the nuclear accumulation of Par3 may be an early event during HGF-induced EMT. It will be interesting and important to determine whether nuclear translocation of Par3 and other polarity proteins occurs under other types of stimuli, such as TGF-β, that are conducive to EMT (Wang *et al*, 2008).

A model for Numb function in HGF-induced EMT

Numb was recently shown to function as a tumour suppressor in breast cancer by protecting p53 from Mdm2-mediated ubiquitination and subsequent degradation, and by antagonizing Notch activity (Frise *et al*, 1996; Pece *et al*, 2004; Leong and Karsan, 2006; Colaluca *et al*, 2008; Dotto, 2008). Our work extends the function of Numb to potentially regulating tumour metastasis by delaying the progression of EMT. This assertion is supported by the observation that depletion of Numb sensitized MDCK cells to HGF-induced cell scattering, reduced cell–cell adhesion, increased cell proliferation and migration. In fact, the migration and proliferation data obtained for the *numb*-shRNA cells is in agreement with recent reports showing that Numb is down-regulated during promoted migration of peripheral glia (Edenfeld *et al*, 2007) and that implantation of *Drosophila* larval neuroblasts carrying a mutation in *numb* triggered tumour growth in the recipient fly (Caussinus and Gonzalez, 2005).

Defects in subcellular localization for E-cad, β-catenin, Par3 and aPKC caused by Numb knockdown suggest an important regulatory role for Numb in cell polarity and cell–cell adhesion. Although there is no direct evidence to support a physical interaction between the AJ and elements

of the Par complex to date, genetic studies have indicated potential interplay between these two cell junctional units. For instance, during *Drosophila* embryogenesis, disruption of the AJ perturbed apical localization of Bazooka (Par3) (Muller and Wieschaus, 1996; Bilder *et al*, 2003). Knockout of α-catenin in mice also led to mislocalization of Par3 and aPKC (Lechler and Fuchs, 2005). On the basis of data presented herein, we propose that Numb is a critical, dynamic link between the TJ and the AJ under physiological and pathological conditions. Under physiological conditions, Numb interacts with both E-cad and Par3 to maintain cell polarity and stabilize cell–cell adhesion. During EMT induced by tyrosine kinase signalling, Numb dissociates from phosphorylated E-cad and Par3, and forms a complex with aPKC–Par6. The formation of the Numb–aPKC–Par6 complex sequesters aPKC–Par6 in the cytoplasm and promotes the dissociation of Par3 from the latter. In the meantime, phosphorylated E-cad and β-catenin are translocated to the apical domain along with reorganization of the actin cytoskeleton to promote cell migration (Supplementary Figure S9). Therefore, Numb likely has a key function in early EMT events when cell–cell adhesion is weakened and cell polarity is lost.

Materials and methods

Peptide array synthesis and probing

Synthesis and probing of peptide-walking array targeting the cytoplasmic domain of human E-cad followed the same procedures as reported earlier (Jia *et al*, 2005).

Antibodies

Antibodies to E-cad (goat, polyclonal), Numb (rabbit, polyclonal), p120-catenin (mouse, monoclonal), aPKC (mouse, monoclonal), Par6 (goat, polyclonal), ZO-1 (goat, polyclonal), c-Src (mouse, monoclonal), Myc (mouse, monoclonal), GFP (rabbit, polyclonal), Na/K-ATPase (mouse, monoclonal), LaminA/C (goat, polyclonal), Tubulin (rabbit, polyclonal) and GST (rabbit, polyclonal) were purchased from Santa Cruz Biotech, Inc (Santa Cruz, CA). An anti-aPKC antibody (rabbit, polyclonal) was purchased from Novus Biologicals, Inc (Littleton, CO). An anti-Par3 antibody (rabbit, polyclonal) and their corresponding antigen (Par3-LTC) were gifts from Dr Zhengjun Chen (Shanghai Institutes for Biological Sciences, China). An anti-β-catenin antibody (rat, monoclonal) was purchased from AbCam Inc (AbCam, MA). Anti-phosphotyrosine (4G10, mouse, polyclonal) and anti-Par3 (rabbit mouse, polyclonal) antibodies were from Upstate Biotech Inc (Upstate, NY). Rhodamine-phalloidin was from Sigma Canada. All antibodies, except for anti-Tubulin (1:300), anti-Par3 (1:500) and anti-Par6 (1:500), were used at a dilution of 1:1000 for western blots. For immunostaining, antibodies were applied at a 1:50 dilution. Fluorescence-conjugated secondary antibodies (Jackson ImmunoResearch, PA) were used at a 1:50 dilution.

Cell culture, IP and western blots

MDCKII cells (obtained from ATCC) and the *ts-src*-MDCKI cells (a gift from Dr Jürgen Behrens, Nikolaus-Fiebiger-Center for Molecular Medicine, Germany) were maintained in DMEM medium supplemented with 10% fetal bovine serum (FBS), 2 mg/ml glutamine and 100 units of penicillin-streptomycin at 37°C. The *ts-src*-MDCKI cells were cultured in 10 cm tissue culture dishes at 40°C for 48 h before transferring to 35°C incubator. For western blots, cells were lysed in RIPA buffer (1% NP40, 0.5% deoxycholate, 150 mM sodium chloride, 25 mM sodium fluoride, 50 mM Tris–HCl, pH 8.0) containing 50 mM phenyl methylsulphonyl fluoride, 2.5 mM sodium orthovanadate 2 mg ml^{-1} aprotinin, 0.1 mg ml^{-1} chymostatin, 1 mg ml^{-1} Chymostatin and 1 mg ml^{-1} pepstatin A. After centrifugation at 13 000 *g* for 20 min, the supernatant was incubated with 5 μl of a specific antibody for 1 h at 4°C. The immunocomplex was precipitated from solution using protein G-Sepharose 4B beads and separated by SDS–polyacrylamide gel electrophoresis. Western blotting was performed by following published procedures (Li *et al*, 2003).

Mutagenesis and sh-RNA-mediated knockdown

E-cad variants containing mutations of Tyr752, TyrY753 or TyrY754 to an Ala or Phe or combinations were generated by site-directed mutagenesis as described (Li *et al*, 2003). The resulting mutants were subcloned into the pEGFP-N1 vector for binding and localization studies. An sh-RNA-mediated knock down strategy was used to deplete Numb from MDCK cells. Specifically, shRNA, 5′-GGACCTCATAGTTGACCAG-3′, directed against specify region of numb gene (Nishimura and Kaibuchi, 2007) was cloned into a pSUPER-GFP/Neo vector (OligoEngine, WA). The transfection of the shRNA into MDCKII cells was carried out using Transfast (Promega, CA) according to the manufacturer's instructions. Four stable *numb*-shRNA MDCK clones were obtained with G418 selection (1 mg/ml, Sigma, Canada). Among them, clone No. 2 was used for all subsequent experiments. For rescue experiments, siRNA-resistant Numb (sr-Numb) was generated by changing the shRNA-targeting sequence to 5′-GGACCTCATTGTAGACCAG-3′ through mutagenesis as described (Nishimura and Kaibuchi, 2007).

Microscopy and confocal microscopy

Phase contrast images of MDCK cells and confocal fluorescent images were acquired on Motic A31 with a 20× phase objective (Motic, Canada) or on a Zeiss LSM 510 META confocal microscope (Carl Zeiss, Germany) with a Zeiss 63× Plan Apochromat oil-immersion objective. Cells were fixed with 4% paraformaldehyde (Sigma, Canada), permeabilized with 0.3% Triton X-100 (Sigma, Canada) and then blocked with 5% BSA (Sigma, Canada) in PBS. The intended primary antibodies (1:50 dilution) were used as described above. The corresponding secondary antibodies (1:50 dilution) conjugated to either FITC (green) or Cy3 (red) were from Jackson ImmunoResearch Lab Inc (Jackson ImmunoResearch, PA). Rhodamine-phalloidin (Sigma, Canada) was used for F-actin staining at 1:50 dilution. Each staining was performed for 1 h at room temperature, which was followed by 3× washes in PBS. Mounting medium with Dapi (Vector Lab Inc, CA) was used to stain nuclei. Confocal Z-stack *x*/*y* plane images were collected with 1-μm interval in a 13 μm total depth. The *x*/*y* or *x*/*z* section images were generated from Z-Stack images with LSM Image software (Carl Zeiss, Germany). Images for direct comparison were obtained under identical parameters and were representative of more than 100 cells in multiple assays.

Cell fractionation

Preparation of cytosol, membrane and nuclear fractions was performed according to the protocol contained in the FractionPREP cell fractionation kit (BioVision Research). The fractionations were confirmed by immunoblotting for Tubulin (a cytosol marker), Na/K-ATPase (a plasma membrane marker) and LaminA/C (a nuclear marker), respectively.

Quantification of data and statistical analysis

Western blots or immunofluorescence images were converted into 8-bit tiff images and then inverted. The background threshold was set by ImageJ (NIH free software) automatically. Subsequently, protein bands or cell–cell junction areas were selected and measured in ImageJ. Statistical analysis was performed with two-tailed Student's *t*-test.

Cell aggregation, wounding, migration and proliferation assays

Cell aggregation assays were performed as described (Thoreson *et al*, 2000) with minor modifications. Briefly, confluent cells were detached from culture dishes using 0.01% trypsin in PBS. After incubating for 1 h at 37°C in a 100 μl overhanging drop on lid, cells were dissociated by pipetting 10 times through a 100-μl tip. For cell wounding and healing assays, MDCKII cells were seeded on 10 cm Petri dishes with 0.5 million cells. Cell at 100% confluency (at approximately 24 h post-seeding) were scratched using a 1000 μl plastic pipette tip and the cell debris were washed away. The plate of cells was then incubated for an indicated period of time in the presence of serum before imaging. The average migration distance in a wounding assay was determined by measuring the gap of the wound at different time points. Boyden chambers cell

migration assay was carried out in Transwell (Corning Inc, NY) 24-well tissue culture plates. The upper chamber was seeded with 1×10^4 cells in serum-free DMEM and incubated overnight. The lower chamber was replaced with 0.5% FBS in DMEM the next day. Cells that migrated to the lower chamber were fixed and stained in Giemsa solution (VWR International, Canada). The migrating cells at the bottom of the filters were counted in four fields per filter in three independent experiments. For cell proliferation assays, aliquots of 1×10^4 cells were seeded into a 96-well plate in quadruplicates and incubated at 37°C for 72 h. At the end of each time point, each well was loaded with 5 μl of fresh MTT (3-(4, 5-dimethylthiazolyl-2)-2,5-diphenyl tetrazolium bromide, 5 mg/ml in PBS, Sigma) and the mixture was incubated for an additional 3 h. The optical absorbance at 570 nm was measured using a 96-well plate ELISA reader. Every MTT assay was conducted in triplicate.

Supplementary data

Supplementary data are available at *The EMBO Journal* Online (http://www.embojournal.org).

Acknowledgements

We thank Dr Jürgen Behrens of Nikolaus-Fiebiger-Center for Molecular Medicine, Germany, for providing the ts-src-MDCKI cells, Dr K Kaibuchi of Nagoya University, Japan, and Dr Zhengjun Chen of Shanghai Institute of Biochemistry and Cell Biology, China, for sharing reagents. This work was supported by grants (to SSCL) from the Canadian Institute of Health Research (CIHR) and Genome Canada through the Ontario Genomic Institute. SSCL holds a Canada Research Chair in Functional Genomics and Cellular Proteomics.

References

Aranda V, Haire T, Nolan ME, Calarco JP, Rosenberg AZ, Fawcett JP, Pawson T, Muthuswamy SK (2006) Par6-aPKC uncouples ErbB2 induced disruption of polarized epithelial organization from proliferation control. *Nat Cell Biol* **8:** 1235–1245

Avizienyte E, Fincham VJ, Brunton VG, Frame MC (2004) Src SH3/2 domain-mediated peripheral accumulation of Src and phospho-myosin is linked to deregulation of E-cadherin and the epithelial-mesenchymal transition. *Mol Biol Cell* **15:** 2794–2803

Avizienyte E, Frame MC (2005) Src and FAK signalling controls adhesion fate and the epithelial-to-mesenchymal transition. *Curr Opin Cell Biol* **17:** 542–547

Avizienyte E, Wyke AW, Jones RJ, McLean GW, Westhoff MA, Brunton VG, Frame MC (2002) Src-induced de-regulation of E-cadherin in colon cancer cells requires integrin signalling. *Nat Cell Biol* **4:** 632–638

Balkovetz DF, Pollack AL, Mostov KE (1997) Hepatocyte growth factor alters the polarity of Madin-Darby canine kidney cell monolayers. *J Biol Chem* **272:** 3471–3477

Behrens J, Vakaet L, Friis R, Winterhager E, Van Roy F, Mareel MM, Birchmeier W (1993) Loss of epithelial differentiation and gain of invasiveness correlates with tyrosine phosphorylation of the E-cadherin/beta-catenin complex in cells transformed with a temperature-sensitive v-SRC gene. *J Cell Biol* **120:** 757–766

Bilder D, Schober M, Perrimon N (2003) Integrated activity of PDZ protein complexes regulates epithelial polarity. *Nat Cell Biol* **5:** 53–58

Birchmeier C, Birchmeier W, Gherardi E, Vande Woude GF (2003) Met, metastasis, motility and more. *Nat Rev Mol Cell Biol* **4:** 915–925

Bose R, Wrana JL (2006) Regulation of Par6 by extracellular signals. *Curr Opin Cell Biol* **18:** 206–212

Boyer B, Roche S, Denoyelle M, Thiery JP (1997) Src and Ras are involved in separate pathways in epithelial cell scattering. *EMBO J* **16:** 5904–5913

Caussinus E, Gonzalez C (2005) Induction of tumor growth by altered stem-cell asymmetric division in Drosophila melanogaster. *Nat Genet* **37:** 1125–1129

Christiansen JJ, Rajasekaran AK (2006) Reassessing epithelial to mesenchymal transition as a prerequisite for carcinoma invasion and metastasis. *Cancer Res* **66:** 8319–8326

Colaluca IN, Tosoni D, Nuciforo P, Senic-Matuglia F, Galimberti V, Viale G, Pece S, Di Fiore PP (2008) NUMB controls p53 tumour suppressor activity. *Nature* **451:** 76–80

Dho SE, Trejo J, Siderovski DP, McGlade CJ (2006) Dynamic regulation of mammalian numb by G protein-coupled receptors and protein kinase C activation: structural determinants of numb association with the cortical membrane. *Mol Biol Cell* **17:** 4142–4155

Dotto GP (2008) Notch tumor suppressor function. *Oncogene* **27:** 5115–5123

Drees F, Pokutta S, Yamada S, Nelson WJ, Weis WI (2005) Alpha-catenin is a molecular switch that binds E-cadherin-beta-catenin and regulates actin-filament assembly. *Cell* **123:** 903–915

Edenfeld G, Altenhein B, Zierau A, Cleppien D, Krukkert K, Technau G, Klambt C (2007) Notch and Numb are required for normal migration of peripheral glia in Drosophila. *Dev Biol* **301:** 27–37

Fang L, Wang Y, Du D, Yang G, Tak Kwok T, Kai Kong S, Chen B, Chen DJ, Chen Z (2007) Cell polarity protein Par3 complexes with DNA-PK via Ku70 and regulates DNA double-strand break repair. *Cell Res* **17:** 100–116

Frise E, Knoblich JA, Younger-Shepherd S, Jan LY, Jan YN (1996) The Drosophila Numb protein inhibits signaling of the Notch receptor during cell-cell interaction in sensory organ lineage. *Proc Natl Acad Sci USA* **93:** 11925–11932

Fujita Y, Krause G, Scheffner M, Zechner D, Leddy HE, Behrens J, Sommer T, Birchmeier W (2002) Hakai, a c-Cbl-like protein, ubiquitinates and induces endocytosis of the E-cadherin complex. *Nat Cell Biol* **4:** 222–231

Guarino M (2007) Epithelial-mesenchymal transition and tumour invasion. *Int J Biochem Cell Biol* **39:** 2153–2160

Guarino M, Rubino B, Ballabio G (2007) The role of epithelial-mesenchymal transition in cancer pathology. *Pathology* **39:** 305–318

Gumbiner BM (2005) Regulation of cadherin-mediated adhesion in morphogenesis. *Nat Rev Mol Cell Biol* **6:** 622–634

Hartsock A, Nelson WJ (2008) Adherens and tight junctions: structure, function and connections to the actin cytoskeleton. *Biochim Biophys Acta* **1778:** 660–669

Hugo H, Ackland ML, Blick T, Lawrence MG, Clements JA, Williams ED, Thompson EW (2007) Epithelial—mesenchymal and mesenchymal—epithelial transitions in carcinoma progression. *J Cell Physiol* **213:** 374–383

Jaffe AB, Hall A (2005) Rho GTPases: biochemistry and biology. *Annu Rev Cell Dev Biol* **21:** 247–269

Jeanes A, Gottardi CJ, Yap AS (2008) Cadherins and cancer: how does cadherin dysfunction promote tumor progression? *Oncogene* **27:** 6920–6929

Jia CY, Nie J, Wu C, Li C, Li SS (2005) Novel Src homology 3 domain-binding motifs identified from proteomic screen of a Pro-rich region. *Mol Cell Proteomics* **4:** 1155–1166

Kametani Y, Takeichi M (2007) Basal-to-apical cadherin flow at cell junctions. *Nat Cell Biol* **9:** 92–98

Kuo CT, Mirzadeh Z, Soriano-Navarro M, Rasin M, Wang D, Shen J, Sestan N, Garcia-Verdugo J, Alvarez-Buylla A, Jan LY, Jan YN (2006) Postnatal deletion of Numb/Numblike reveals repair and remodeling capacity in the subventricular neurogenic niche. *Cell* **127:** 1253–1264

Le TL, Yap AS, Stow JL (1999) Recycling of E-cadherin: a potential mechanism for regulating cadherin dynamics. *J Cell Biol* **146:** 219–232

Lechler T, Fuchs E (2005) Asymmetric cell divisions promote stratification and differentiation of mammalian skin. *Nature* **437:** 275–280

Leong KG, Karsan A (2006) Recent insights into the role of Notch signaling in tumorigenesis. *Blood* **107:** 2223–2233

Levayer R, Lecuit T (2008) Breaking down EMT. *Nat Cell Biol* **10:** 757–759

Li C, Iosef C, Jia CY, Han VK, Li SS (2003) Dual functional roles for the X-linked lymphoproliferative syndrome gene product SAP/SH2D1A in signaling through the signaling lymphocyte activation molecule (SLAM) family of immune receptors. *J Biol Chem* **278:** 3852–3859

Lilien J, Balsamo J (2005) The regulation of cadherin-mediated adhesion by tyrosine phosphorylation/dephosphorylation of beta-catenin. *Curr Opin Cell Biol* **17:** 459–465

Lupher Jr ML, Songyang Z, Shoelson SE, Cantley LC, Band H (1997) The Cbl phosphotyrosine-binding domain selects a D(N/D)XpY motif and binds to the Tyr292 negative regulatory phosphorylation site of ZAP-70. *J Biol Chem* **272:** 33140–33144

Macara IG (2004) Parsing the polarity code. *Nat Rev Mol Cell Biol* **5:** 220–231

Mandal M, Myers JN, Lippman SM, Johnson FM, Williams MD, Rayala S, Ohshiro K, Rosenthal DI, Weber RS, Gallick GE, El-Naggar AK (2008) Epithelial to mesenchymal transition in head and neck squamous carcinoma: association of Src activation with E-cadherin down-regulation, vimentin expression, and aggressive tumor features. *Cancer* **112:** 2088–2100

Margolis B, Borg JP (2005) Apicobasal polarity complexes. *J Cell Sci* **118:** 5157–5159

Matter K, Balda MS (2003) Functional analysis of tight junctions. *Methods* **30:** 228–234

McCleverty CJ, Lin DC, Liddington RC (2007) Structure of the PTB domain of tensin1 and a model for its recruitment to fibrillar adhesions. *Protein Sci* **16:** 1223–1229

Muller HA, Wieschaus E (1996) Armadillo, bazooka, and stardust are critical for early stages in formation of the zonula adherens and maintenance of the polarized blastoderm epithelium in Drosophila. *J Cell Biol* **134:** 149–163

Nishimura T, Kaibuchi K (2007) Numb controls integrin endocytosis for directional cell migration with aPKC and PAR-3. *Dev Cell* **13:** 15–28

Ozdamar B, Bose R, Barrios-Rodiles M, Wang HR, Zhang Y, Wrana JL (2005) Regulation of the polarity protein Par6 by TGFbeta receptors controls epithelial cell plasticity. *Science* **307:** 1603–1609

Palovuori R, Sormunen R, Eskelinen S (2003) SRC-induced disintegration of adherens junctions of madin-darby canine kidney cells is dependent on endocytosis of cadherin and antagonized by Tiam-1. *Lab Invest* **83:** 1901–1915

Pece S, Gutkind JS (2002) E-cadherin and Hakai: signalling, remodeling or destruction? *Nat Cell Biol* **4:** E72–E74

Pece S, Serresi M, Santolini E, Capra M, Hulleman E, Galimberti V, Zurrida S, Maisonneuve P, Viale G, Di Fiore PP (2004) Loss of negative regulation by Numb over Notch is relevant to human breast carcinogenesis. *J Cell Biol* **167:** 215–221

Ponzetto C, Bardelli A, Zhen Z, Maina F, dalla Zonca P, Giordano S, Graziani A, Panayotou G, Comoglio PM (1994) A multifunctional docking site mediates signaling and transformation by the hepatocyte growth factor/scatter factor receptor family. *Cell* **77:** 261–271

Rasin MR, Gazula VR, Breunig JJ, Kwan KY, Johnson MB, Liu-Chen S, Li HS, Jan LY, Jan YN, Rakic P, Sestan N (2007) Numb and Numbl are required for maintenance of cadherin-based adhesion and polarity of neural progenitors. *Nat Neurosci* **10:** 819–827

Richardson JC, Scalera V, Simmons NL (1981) Identification of two strains of MDCK cells which resemble separate nephron tubule segments. *Biochim Biophys Acta* **673:** 26–36

Roncarati R, Sestan N, Scheinfeld MH, Berechid BE, Lopez PA, Meucci O, McGlade JC, Rakic P, D'Adamio L (2002) The gamma-secretase-generated intracellular domain of beta-amyloid precursor protein binds Numb and inhibits Notch signaling. *Proc Natl Acad Sci USA* **99:** 7102–7107

Santolini E, Puri C, Salcini AE, Gagliani MC, Pelicci PG, Tacchetti C, Di Fiore PP (2000) Numb is an endocytic protein. *J Cell Biol* **151:** 1345–1352

Shin K, Fogg VC, Margolis B (2006) Tight junctions and cell polarity. *Annu Rev Cell Dev Biol* **22:** 207–235

Smith CA, Lau KM, Rahmani Z, Dho SE, Brothers G, She YM, Berry DM, Bonneil E, Thibault P, Schweisguth F, Le Borgne R, McGlade CJ (2007) aPKC-mediated phosphorylation regulates asymmetric membrane localization of the cell fate determinant Numb. *EMBO J* **26:** 468–480

Suzuki A, Ohno S (2006) The PAR-aPKC system: lessons in polarity. *J Cell Sci* **119:** 979–987

Thiery JP, Sleeman JP (2006) Complex networks orchestrate epithelial-mesenchymal transitions. *Nat Rev Mol Cell Biol* **7:** 131–142

Thoreson MA, Anastasiadis PZ, Daniel JM, Ireton RC, Wheelock MJ, Johnson KR, Hummingbird DK, Reynolds AB (2000) Selective uncoupling of p120(ctn) from E-cadherin disrupts strong adhesion. *J Cell Biol* **148:** 189–202

Vasioukhin V, Bauer C, Yin M, Fuchs E (2000) Directed actin polymerization is the driving force for epithelial cell-cell adhesion. *Cell* **100:** 209–219

Wang Q, Hurd TW, Margolis B (2004) Tight junction protein Par6 interacts with an evolutionarily conserved region in the amino terminus of PALS1/stardust. *J Biol Chem* **279:** 30715–30721

Wang Q, Margolis B (2007) Apical junctional complexes and cell polarity. *Kidney Int* **72:** 1448–1458

Wang X, Nie J, Zhou Q, Liu W, Zhu F, Chen W, Mao H, Luo N, Dong X, Yu X (2008) Downregulation of Par-3 expression and disruption of Par complex integrity by TGF-beta during the process of epithelial to mesenchymal transition in rat proximal epithelial cells. *Biochim Biophys Acta* **1782:** 51–59

Wang Y, Du D, Fang L, Yang G, Zhang C, Zeng R, Ullrich A, Lottspeich F, Chen Z (2006) Tyrosine phosphorylated Par3 regulates epithelial tight junction assembly promoted by EGFR signaling. *EMBO J* **25:** 5058–5070

White WO, Seibenhener ML, Wooten MW (2002) Phosphorylation of tyrosine 256 facilitates nuclear import of atypical protein kinase C. *J Cell Biochem* **85:** 42–53

Yamada S, Pokutta S, Drees F, Weis WI, Nelson WJ (2005) Deconstructing the cadherin-catenin-actin complex. *Cell* **123:** 889–901

Yang J, Weinberg RA (2008) Epithelial-mesenchymal transition: at the crossroads of development and tumor metastasis. *Dev Cell* **14:** 818–829

Zwahlen C, Li SC, Kay LE, Pawson T, Forman-Kay JD (2000) Multiple modes of peptide recognition by the PTB domain of the cell fate determinant Numb. *EMBO J* **19:** 1505–1515